TU Delft

Delft University of Technology

Observation of a Giant Goos-Hänchen Shift for Matter Waves

McKay, S.; De Haan, V. O.; Leiner, J.; Parnell, S. R.; Dalgliesh, R. M.; Boeni, P.; Bannenberg, L. J.; Le Thien, Q.; Pynn, R.; More Authors

DOI
10.1103/PhysRevLett.134.093803

Publication date
2025

Document Version
Final published version

Published in
Physical review letters

Citation (APA)
McKay, S., De Haan, V. O., Leiner, J., Parnell, S. R., Dalgliesh, R. M., Boeni, P., Bannenberg, L. J., Le Thien, Q., Pynn, R., & More Authors (2025). Observation of a Giant Goos-Hänchen Shift for Matter Waves. *Physical review letters*, *134*(9), Article 093803. https://doi.org/10.1103/PhysRevLett.134.093803

Important note
To cite this publication, please use the final published version (if applicable).
Please check the document version above.

Copyright
Other than for strictly personal use, it is not permitted to download, forward or distribute the text or part of it, without the consent of the author(s) and/or copyright holder(s), unless the work is under an open content license such as Creative Commons.

Takedown policy
Please contact us and provide details if you believe this document breaches copyrights.
We will remove access to the work immediately and investigate your claim.

This work is downloaded from Delft University of Technology.
For technical reasons the number of authors shown on this cover page is limited to a maximum of 10.

Green Open Access added to TU Delft Institutional Repository

'You share, we take care!' - Taverne project

https://www.openaccess.nl/en/you-share-we-take-care

Otherwise as indicated in the copyright section: the publisher is the copyright holder of this work and the author uses the Dutch legislation to make this work public.

Observation of a Giant Goos-Hänchen Shift for Matter Waves

S. McKay,[1,2] V. O. de Haan,[3] J. Leiner,[4] S. R. Parnell,[5,6] R. M. Dalgliesh,[6] P. Boeni,[7,8] L. J. Bannenberg,[5] Q. Le Thien,[1] D. V. Baxter,[1,2,9] G. Ortiz,[1,9,10,11] and R. Pynn[1,2,4,9,*]

[1]*Department of Physics, Indiana University, Bloomington, Indiana 47405, USA*
[2]*Center for Exploration of Energy and Matter, Indiana University, Bloomington, Indiana 47408, USA*
[3]*BonPhysics Research and Investigations BV, Laan van Heemstede 38, 3297AJ Puttershoek, The Netherlands*
[4]*Neutron Sciences Directorate, Oak Ridge National Laboratory, Oak Ridge, Tennessee 37830, USA*
[5]*Faculty of Applied Sciences, Delft University of Technology, Mekelweg 15, 2629 JB Delft, The Netherlands*
[6]*ISIS, Rutherford Appleton Laboratory, Chilton, Oxfordshire OX11 0QX, United Kingdom*
[7]*Physics Department E21, Technical University of Munich, D-85748 Garching, Germany*
[8]*SwissNeutronics AG, Brühlstrasse 28, CH-5313 Klingnau, Switzerland*
[9]*Quantum Science and Engineering Center, Indiana University, Bloomington, Indiana 47408, USA*
[10]*Institute for Advanced Study, Princeton, New Jersey 08540, USA*
[11]*Institute for Quantum Computing, University of Waterloo, Waterloo, N2L 3G1, ON, Canada*

(Received 5 July 2024; accepted 27 January 2025; published 5 March 2025)

The Goos-Hänchen (GH) shift describes a phenomenon in which a specularly reflected beam is translated along the reflecting surface such that the incident and reflected rays no longer intersect at the surface. Using a neutron spin-echo technique and a specially designed magnetic multilayer mirror, we have measured the relative phase between the reflected up and down neutron spin states in total reflection. The relative GH shift calculated from this phase shows a strong resonant enhancement at a particular incident neutron wave vector, which is due to a waveguiding effect in one of the magnetic layers. Calculations based on the observed phase difference between the neutron states indicate a propagation distance along the waveguide layer of 0.65 mm for the spin-down state, which we identify with the magnitude of the giant GH shift. The existence of a physical GH shift is confirmed by the observation of neutron absorption in the waveguide layer. We propose ways in which our experimental method may be exploited for neutron quantum-enhanced sensing of thin magnetic layers.

DOI: 10.1103/PhysRevLett.134.093803

Introduction—The Goos-Hänchen (GH) shift, in which incident and reflected rays do not exactly intersect at the reflecting surface, was first experimentally confirmed for light in 1947 [1,2]. Although the longitudinal GH shift for light beams is often of similar magnitude to the wavelength of the light used, much larger shifts as large as 1 mm, dubbed *giant GH shifts*, have recently been calculated for resonant structures [3] and are now proposed as the basis for ultrasensitive devices for measuring temperature [4] and relative humidity [5]. The electron GH effect is also being investigated for its potential application in semiconductors and graphene-based nanostructures [6].

About a decade ago, de Haan *et al.* [7] attempted to confirm the existence of the GH effect for neutrons, the first type of matter waves to be explored. Using the technique of neutron spin echo, they measured the difference in phase between the up and down neutron spin states reflected from a magnetic mirror made of Permalloy. Unfortunately, the phase difference in this case was small, and critics suggested that the experimental result could have been caused by neutron depolarization [8,9]. Furthermore, critics noted that the phase difference between states is not a direct confirmation of the relative GH spatial shift of the neutron spin states, which must be inferred from theory when only the relative phases are measured. Theory predicted a maximum GH shift of 2.8 μm for the experiment reported in [7]. Several theoretical studies of the GH effect for neutrons have been published [10–12], at least one of which [11] proposed increasing the magnitude of the effect by using multilayered magnetic structures; we have adopted this approach using a specially designed multilayer.

Sample design and experiment—The composition of our multilayer, fabricated by Swiss Neutrons AG, is shown in Fig. 1 and Table I. Vacoflux 50©, a commercially available FeCoV alloy (Vacuumschmelze GmbH & Co. KG) with an elemental composition of 49% Fe, 49% Co, and 2% V by weight, has two important properties. First, it is magnetically soft and, when deposited in a manner introducing appropriate strain, can be magnetized by a modest 20 mT magnetic field along an in-plane easy axis, remaining fully magnetized when removed from the field [13]. Second, the composition of Vacoflux leads to a neutron scattering

*Contact author: rpynn@iu.edu

 © 2025 American Physical Society

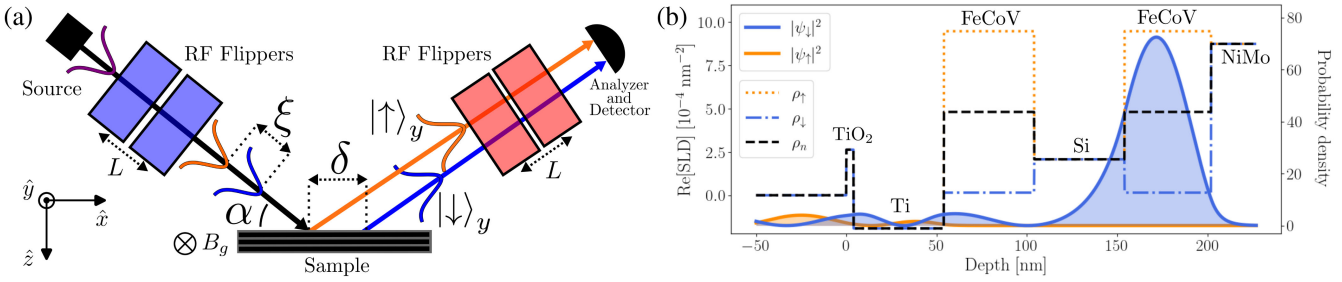

FIG. 1. (a) Sketch of the experimental setup. The neutron (purple) initially polarized in the $(|\uparrow\rangle_y + |\downarrow\rangle_y)/\sqrt{2}$ state is spin-path entangled by the first set of radio-frequency (rf) flippers, resulting in an incident state with a wavepacket separation ξ. During reflection, the spin-up (orange) and spin-down (blue) state experience a different GH shift; the relative GH shift is labeled δ. Finally, the second pair of flippers disentangles the reflected state, which recombines the two wavepackets (producing a neutron spin echo when the reflecting sample is non-magnetic). The composition of the multilayer sample is displayed in Table I. Experiments were performed with the magnetization of the sample in the $\hat{x}$ and $\hat{y}$ directions. The weak guide field at the sample position is labeled B_g. The incident grazing angle α, GH shift, and wavepacket separation are all exaggerated for clarity. (b) Calculated probability densities of both spin states $|\psi_i|^2$ with $i \in \{\uparrow, \downarrow\}$ (with $\hat{y}$ as the quantization axis) in the various layers relative to an incident planewave state with unit amplitude, $\lambda = 0.9$ nm, and $\alpha = 0.34°$ using the optical transfer matrix formalism [17]. There is a strong resonance of the spin-down state in the lower FeCoV layer while the spin-up state has negligible probability density beyond the Ti layer. The spin-up, spin-down, and nuclear SLDs are labeled $\rho_\uparrow$, $\rho_\downarrow$, and ρ_n, respectively.

length density (SLD) that is close to zero for spin-down neutrons whose magnetic moments are aligned with the magnetization direction in the alloy layer. The NiMo layer contains $9.7 \pm 1.5\%$ Mo (atomic percent), which is sufficient to ensure that there is no magnetic neutron scattering from this layer [14]. Because the Vacoflux layer closest to the substrate has positive SLD layers on either side (Si above and NiMo below), we anticipate a waveguiding, or Fabry-Pérot, effect for spin-down neutrons in this layer and no such effect for spin-up neutrons [15,16].

A sketch of the experimental geometry is shown in Fig. 1(a). Our entangled-neutron reflection experiment used the Larmor beamline at the ISIS neutron and muon source in the United Kingdom. Two radio-frequency (rf) neutron spin flippers separated by a distance of ~1.5 m operating at a frequency of 1 MHz with the boundaries of their static magnetic fields perpendicular to the direction of neutron travel were used to mode-entangle (i.e., intraparticle entangle) the spin and path states of the incident neutrons [18–20]. The two flippers before the sample induce a phase difference between the neutron spin states, which is reversed by two similar flippers after the scattering sample, thereby producing a neutron spin echo when the reflecting sample is nonmagnetic [21]. This relative phase θ_k, commonly called the *Larmor phase*, is given by $\theta_k = \boldsymbol{k} \cdot \boldsymbol{\xi} = 2fm\lambda L/\hbar$, where the *entanglement length* $\xi = |\boldsymbol{\xi}|$ is the wavelength-dependent spatial separation of the two entangled spin states after exiting the second rf flipper, $\boldsymbol{k} = (k_x, k_y, k_z)$ the neutron wave vector, f the rf frequency, m the mass of the neutron, L the distance between each pair of rf flippers, and λ the neutron wavelength [22]. For all measurements in this experiment, the spatial separation of the spin states was purely along the direction of travel $\hat{k}$ of the neutron, and the wavelength-dependent Larmor phase was fixed to $\theta_k \approx [4.8 \times 10^4 \text{ nm}^{-1}]\lambda$, which also fixes $\xi \approx [7.6 \times 10^3 \text{ nm}^{-1}]\lambda^2$.

The premagnetized multilayer was mounted in reflection geometry with its magnetization $\boldsymbol{M}_{\text{sam}}$ either parallel or perpendicular to a weak (~0.5 mT) magnetic guide field $\boldsymbol{B}_g = -B_g\hat{y}$ used to define the quantization axis for the neutron spins. This field had no effect on the sample magnetization. A grazing incidence angle of $\alpha = 0.34 \pm 0.02°$ was used during the experiment, ensuring that neutrons with $\lambda \gtrsim 0.4$ nm fell within the region of total external reflection of the multilayer. A supermirror bender with its blades parallel to the neutron scattering plane of the experiment was used as a polarization analyzer and a linear, scintillation-based, position-sensitive, neutron detector with a 1D pixel size of 0.64 mm in the neutron scattering plane was used. The neutron beam dimension

TABLE I. Table of nominal layer thicknesses and nuclear (ρ_n), magnetic (ρ_m), and imaginary (Im[ρ]) scattering length densities of the sample. The non-magnetic sample used for normalization of the echo polarization consisted of a 100 nm thick NiMo layer on a Si substrate. The SLDs of the FeCoV layers were calculated assuming 95% bulk density and 92% of the bulk magnetic saturation (1.8×10^7 A m^{-1}).

Material	Thickness (nm)	ρ_n 10^{-4} nm^{-2}	ρ_m 10^{-4} nm^{-2}	$-$Im[ρ] 10^{-7} nm^{-2}
TiO_2	4	2.63	0	0.54
Ti	50	−1.91	0	0.96
FeCoV	50	4.81	4.66	4.5
Si	50	2.07	0	0.024
FeCoV	50	4.81	4.66	4.5
NiMo	100	8.73	0	1.0
Si	Substrate	2.07	0	0.024

perpendicular to the scattering plane was 20 mm. Two slits defined the width of the observed neutron beam in the $\hat{z}$ direction of Fig. 1(a); the first 0.5 mm wide slit was positioned 25 cm before the sample and the second 2 mm wide slit 35 cm behind the sample to limit background scattering. The spin echo was established using a reflecting sample consisting of a 100 nm layer of NiMo on a silicon substrate; the NiMo composition and substrate dimension were identical to that used for the multilayer sample.

For values of the component $k_z = (2\pi/\lambda)\sin\alpha$ of the neutron wave vector perpendicular to the reflecting surface of a sample that are below the critical values for the spin states, neutrons are usually totally externally reflected. For both measurements of our multilayer in the parallel ($\boldsymbol{M}_{\rm sam} \parallel \boldsymbol{B}_g$) and perpendicular ($\boldsymbol{M}_{\rm sam} \perp \boldsymbol{B}_g$) orientations, the incident neutron state is given by $|\psi_{\rm in}\rangle = (e^{-i\theta_k/2}|\uparrow\rangle_y + e^{i\theta_k/2}|\downarrow\rangle_y)/\sqrt{2}$. After reflection, the neutron state is determined by the application of the appropriate optical transfer matrix $\mathbf{M}$:

$$\mathbf{M}^{\parallel} = \mathrm{diag}(r_\uparrow e^{i\phi_\uparrow}, r_\downarrow e^{i\phi_\downarrow}), \qquad \mathbf{M}^{\perp} = \mathcal{U}^\dagger \mathbf{M}^{\parallel} \mathcal{U}, \quad (1)$$

where $\mathcal{U}$ is the appropriate change-of-basis matrix and $r_\uparrow e^{i\phi_\uparrow}$ and $r_\downarrow e^{i\phi_\downarrow}$ are the complex reflectances for the spin-up and -down states, respectively. The reflectances for each spin state can be calculated using the standard optical transfer matrix formalism [17], and the general framework of Ref. [23] was utilized to analyze measurements in the spin-echo modality [24].

Assuming perfect beam polarization, when the magnetization of the sample is parallel to the magnetic guide field at the sample position, the experimentally measured spin echo polarization $P_z^{\parallel}$ and reflectivity $R^{\parallel}$ are given in the plane-wave limit by

$$P_z^{\parallel} = \frac{2r_\uparrow r_\downarrow}{r_\uparrow^2 + r_\downarrow^2}\cos(\phi_\uparrow - \phi_\downarrow), \qquad R^{\parallel} = \frac{r_\uparrow^2 + r_\downarrow^2}{2}. \quad (2)$$

The Larmor phase θ_k varies extremely rapidly with neutron wavelength at an rf frequency of 1 MHz, and we lack the wavelength resolution ($\sim 5 \times 10^{-3}$ nm) to resolve such a rapidly oscillating phase [24]. Therefore, the polarization and reflectivity in the perpendicular case become

$$P_z^{\perp} = \frac{2r_\uparrow r_\downarrow}{(r_\uparrow + r_\downarrow)^2}[1 + \cos(\phi_\uparrow - \phi_\downarrow)], \qquad R^{\perp} = R^{\parallel}. \quad (3)$$

Because the measured polarization contains the phase information from the spin states, we can extract the GH shift. According to the Artmann-Carter-Hora (ACH) theory of the GH shift, the GH shift for each spin state is given by $\delta_i = (\partial\phi_i/\partial k_z)\cot\alpha$, where ϕ_i for $i \in \{\uparrow, \downarrow\}$ is the phase of the neutron [33,34]. As our experiment is only sensitive to the relative GH shift between the two spin states, we also define the relative GH shift as $\delta = \delta_\downarrow - \delta_\uparrow$, which is shown in Fig. 1(a).

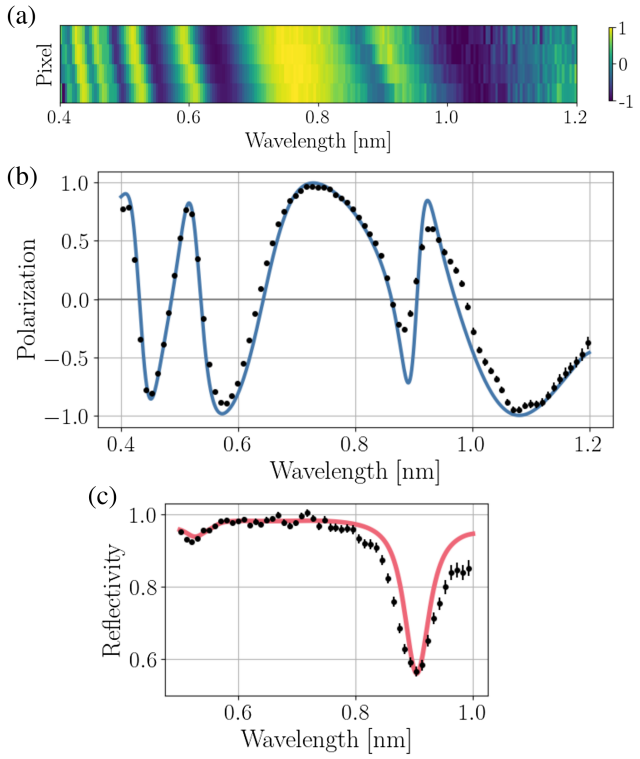

FIG. 2. (a) False color plot of the observed neutron polarization plotted against detector pixel and neutron wavelength for the sample magnetization parallel to the guide field $\boldsymbol{B}_g$ [c.f. Fig. 1(a)]. (b) Measured polarization $P_z^{\parallel}$ summed over the detector at constant momentum transfer. The blue curve represents the polarization from a transfer matrix simulation described in the text. Notice that the polarization ranges from -1 to 1. (c) Measured sum of up- and down-spin state reflectivity $R^{\parallel}$. The red curve shows the result of the same simulation but with $\mathrm{Im}[\rho]$ in the second FeCoV layer increased by a factor of 7.5 from the table value.

Results—Even though the incident neutron beam in our experiment was well-collimated in the scattering plane, its angular divergence covered several detector pixels as shown in the false-color plot of echo polarization versus pixel and neutron wavelength λ shown in Figs. 2(a) and 3(a). Summing the measured neutron intensity at constant momentum transfer leads to the plots of echo polarization versus λ shown in Figs. 2(b) and 3(b) for two orientations of the sample magnetization.

The curves in Figs. 2(b) and 3(b) represent a transfer matrix simulation convolved with the angular divergence of the neutron beam implied by the pixel size of the detector and the footprint of the neutron beam on the sample. These simulations use the SLDs and layer thicknesses given in Table I, except for the case of the lower FeCoV layer, where we find a slightly better fit to the data with a thickness of 48 nm instead of the nominal 50 nm. For the most part, the

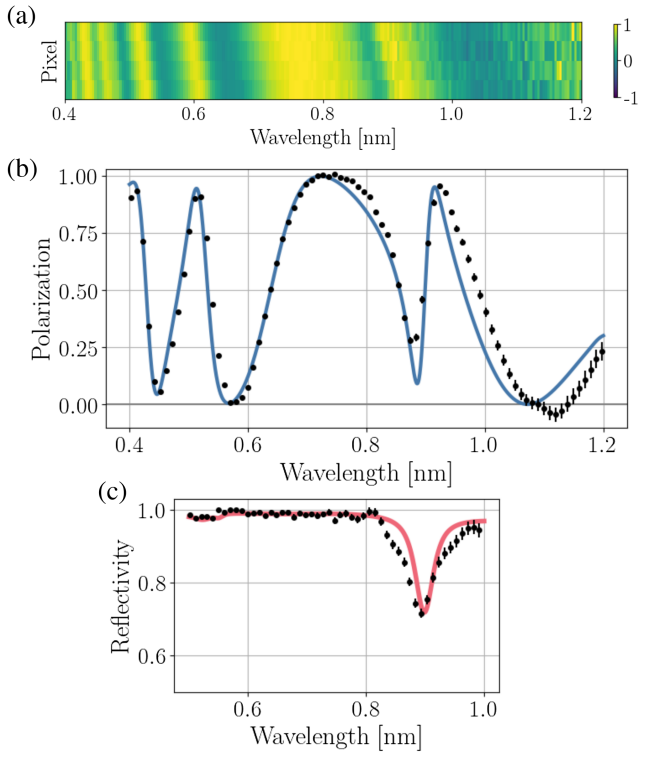

FIG. 3. Similar plot as Fig. 2 for (a) and (b) $P_z^{\perp}$ and (c) $R^{\perp}$. Notice in (b) that the polarization ranges from 0 to 1. In (c), Im$[\rho]$ in the second FeCoV layer was increased by a factor of 2.5 from the table value.

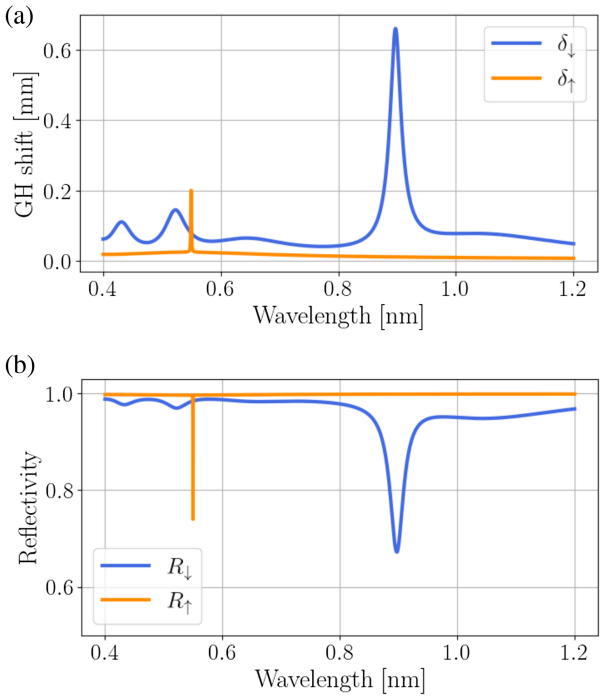

FIG. 4. (a) Calculated values of the GH shifts using the ACH formula for the up (orange) and down (blue) neutron spin states. (b) Calculated reflectivities $R_\uparrow$ and $R_\downarrow$. For both (a) and (b), a grazing incidence angle of $\alpha = 0.34°$ is used and absorption is included using the values of Im$[\rho]$ displayed in Table I. The correlation between the dip in reflectivity and the large GH shift is discussed in Ref. [24].

echo polarization is not particularly sensitive to the precise values of the SLDs given in Table I. The exception to this rule is the spin-down SLD of the lower FeCoV layer which determines the position of the sharp structure that occurs around 0.9 nm in Figs. 2(c) and 3(c). The value given in Table I is slightly less (92%) than would be obtained using the bulk saturation magnetization of Vacoflux and has been chosen to give the correct position of the sharp jump in the echo polarization. Between the two data sets, only α has been slightly adjusted by less than 0.01°, within the potential error made in remounting the sample. The GH shifts for up and down states calculated from the parameters of our multilayer are plotted for both spin states in Fig. 4(a), showing a very large resonance for the down-spin state at $k_z = 0.04$ nm^{-1} corresponding to $\lambda = 0.9$ nm at a grazing angle of incidence of $\alpha = 0.34°$. At its peak, this resonance corresponds to a calculated GH shift of $\delta_\downarrow \approx 0.65$ mm. The calculated GH shift for the spin-up state is negligible for $\lambda \gtrsim 0.6$ nm, so we can approximate $\delta \approx \delta_\downarrow$.

While the measurement of the relative phases between the two states, taken together with the traditional ACH theory of the GH effect, predicts a giant GH shift for the down-spin state, the experiment as described so far does not directly detect the shift. However, Vacoflux contains a substantial fraction (49%) of cobalt which has a relatively large neutron absorption cross section. When this is included in the simulation, there is a significant change in the calculated reflectivity for the spin-down state with no change for the spin-up state as shown in Fig. 4(b). Simulations verify that the lower FeCoV layer is the main contributor to the change in the down-state reflectivity. The reason that the lower FeCoV layer plays this important role is suggested by Fig. 1(b): the down-state SLD for FeCoV is close to zero and the lower FeCoV layer is surrounded on both sides by layers with positive SLDs. Thus, the lower FeCoV layer acts as a trapping potential for neutrons which are waveguided within this layer, parallel to the sample surface. Because down-state neutrons see the lower FeCoV layer as a waveguide, they can be absorbed by the cobalt nuclei in this layer as they travel in the layer parallel to the sample surface. The resonant dip in the reflectivity of the down state corresponds to greatly increased absorption which, in turn, occurs because neutrons travel a large distance in the lower FeCoV layer. The observation of the resonant dip in reflectivity in the critical region is thus direct evidence for a GH shift in our multilayer.

Figures 2(c) and 3(c) show plots of the sum of the measured up- and down-state reflectivities for our multilayer normalized to the average simulated values for wavelengths between 0.6 nm and 0.75 nm. The deep resonant dips corresponding to the giant GH shift are clear

although the magnitudes of the dips depend on sample orientation. To account for the observed depth of the dip using the transfer matrix simulation, we need to increase $\mathrm{Im}[\rho]$ in the lower FeCoV layer from the table value of -4.5×10^{-7} to -3.4×10^{-6} nm^{-2} when the sample magnetization is parallel to the magnetic guide field and to a value of -1.1×10^{-6} nm^{-2} in the perpendicular-magnetization case. Thus, while the dip in the reflectivity is a direct manifestation of the GH shift, its magnitude is not described by the standard optical theory incorporating neutron absorption alone. However, as Sears [35] has pointed out, $\mathrm{Im}[\rho]$ should include all channels which cause neutrons to be "lost," including both coherent and incoherent scattering in addition to absorption. Since the known incoherent scattering of FeCoV is small, we conclude that there is significant neutron scattering within the lower FeCoV layer and that this scattering depends on the direction in which the waveguided neutron travels in the layer. This is hardly surprising given the manner in which the layer is intentionally strained during deposition in order to create a preferred direction for remanent magnetization. Significant small angle scattering, attributed to uncorrelated magnetic domains, has been reported for multilayers in which one component was an FeCoV layer of slightly different composition than that used in our experiment [36].

Conclusion—In conclusion, we have provided strong experimental evidence for a giant Goos-Hänchen shift for neutron matter waves. The measured phase difference between up- and down-state reflected neutrons is well-described by the usual optical transfer matrix formalism, and the existence of a resonant dip in the reflectivity below the critical reflection wave vector confirms that down-state neutrons have an extended dwell time in our multilayer sample and thus a concomitant large GH shift [24]. Based on the agreement of the measured relative phases and the standard optical theory we can use the ACH theory to estimate the GH shift as 0.65 mm.

Finally, we note that measurements of the phase difference between up and down neutron spin states reflected from magnetic layered systems may be useful for some applications. For example, in entangled-beam reflectometry [23] the phase difference can be measured for very thin and weakly magnetic layers below the critical angle where the reflectivity is unity for both neutron states. Standard spin asymmetry measurements used in polarized neutron reflectometry may be very hard to apply for such samples because the asymmetry occurs only at high momentum transfers where the reflectivity is very low. Thus, we conjecture that phase measurements below the critical edge may be exploited for enhanced quantum sensing of magnetism in two-dimensional systems.

Acknowledgments—The IU Quantum Science and Engineering Center is supported by the Office of the IU Bloomington Vice Provost for Research through its Emerging Areas of Research program. Some of this work was supported by the Department of Commerce through Cooperative Agreement No. 70NANB15H259. The experiment was performed on the Larmor instrument at the ISIS Neutron and Muon source (UK) supported by a beam time allocation RB2310496 from the Science and Technology Facilities Council [37]. We would like to thank Amy Navarathna from the TU Delft for performing the X-ray reflectometry measurements. This research was undertaken thanks in part to funding from the Canada First Research Excellence Fund. G. O. gratefully acknowledges support from the Institute for Advanced Study. Q. L. T. would like to thank Dennis Krause for pointing out the connection of this work with interferometry of unstable particles.

[1] F. Goos and H. Hänchen, Ann. Phys. (Berlin) **435**, 383 (1943).
[2] F. Goos and H. Hänchen, Ann. Phys. (Berlin) **436**, 333 (1947).
[3] F. Wu, J. Wu, Z. Guo, H. Jiang, Y. Sun, Y. Li, J. Ren, and H. Chen, Phys. Rev. Appl. **12**, 014028 (2019).
[4] X. Zhou, P. Tang, C. Yang, S. Liu, and Z. Luo, Results Phys. **24**, 104100 (2021).
[5] X. Wang, M. Sang, W. Yuan, Y. Nie, and H. Luo, IEEE Photonics Technol. Lett. **28**, 264 (2016).
[6] X. Chen, X.-J. Lu, Y. Ban, and C.-F. Li, J. Opt. **15**, 033001 (2013).
[7] V. O. de Haan, J. Plomp, T. M. Rekveldt, W. H. Kraan, A. A. van Well, R. M. Dalgliesh, and S. Langridge, Phys. Rev. Lett. **104**, 010401 (2010).
[8] V. K. Ignatovich, Phys. Rev. Lett. **105**, 018901 (2010).
[9] V. O. De Haan, J. Plomp, T. M. Rekveldt, W. H. Kraan, A. A. Van Well, R. M. Dalgliesh, and S. Langridge, Phys. Rev. Lett. **105**, 018902 (2010).
[10] V. Ignatovich, Phys. Lett. A **322**, 36 (2004).
[11] A. I. Frank, J. Phys. Conf. Ser. **528**, 012029 (2014).
[12] V. A. Bushuev and A. I. Frank, Phys. Usp. **61**, 952 (2018).
[13] D. Clemens, A. Vananti, C. Terrier, P. Böni, B. Schnyder, S. Tixier, and M. Horisberger, Physica (Amsterdam) **234–236B**, 500 (1997).
[14] J. Padiyath, J. Stahn, P. Allenspach, M. Horisberger, and P. Böni, Physica (Amsterdam) **350B**, E237 (2004).
[15] R. E. De Wames and S. K. Sinha, Phys. Rev. B **7**, 917 (1973).
[16] Y. P. Feng, C. F. Majkrzak, S. K. Sinha, D. G. Wiesler, H. Zhang, and H. W. Deckman, Phys. Rev. B **49**, 10814 (1994).
[17] L. G. Parratt, Phys. Rev. **95**, 359 (1954).
[18] J. Shen, S. J. Kuhn, R. M. Dalgliesh, V. O. de Haan, N. Geerits, A. A. M. Irfan, F. Li, S. Lu, S. R. Parnell, J. Plomp, A. A. van Well, A. Washington, D. V. Baxter, G. Ortiz, W. M. Snow, and R. Pynn, Nat. Commun. **11**, 930 (2020).
[19] S. J. Kuhn, S. McKay, J. Shen, N. Geerits, R. M. Dalgliesh, E. Dees, A. A. M. Irfan, F. Li, S. Lu, V. Vangelista, D. V. Baxter, G. Ortiz, S. R. Parnell, W. M. Snow, and R. Pynn, Phys. Rev. Res. **3**, 023227 (2021).
[20] J. C. Leiner, S. J. Kuhn, S. McKay, J. K. Jochum, F. Li, A. A. M. Irfan, F. Funama, D. Mettus, L. Beddrich, C. Franz, J. Shen, S. R. Parnell, R. M. Dalgliesh, M. Loyd, N. Geerits, G. Ortiz, C. Pfleiderer, and R. Pynn, Phys. Rev. Appl. **22**, L031005 (2024).

[21] F. Mezei, Z. Phys. A Hadrons Nucl. **255**, 146 (1972).
[22] R. Golub and R. Gähler, Phys. Lett. **123A**, 43 (1987).
[23] Q. Le Thien, R. Pynn, and G. Ortiz, preceding Letter, Phys. Rev. Lett. **134**, 093802 (2025).
[24] See Supplemental Material at http://link.aps.org/supplemental/10.1103/PhysRevLett.134.093803, which includes Refs. [25–32], for the x-ray reflectometry characterization of the multilayer, a description of the neutron reflectometery data treatment, a discussion of the neutron dwell time in the multilayer, and theoretical methods.
[25] A. Glavic and M. Björck, J. Appl. Crystallogr. **55**, 1063 (2022).
[26] F. Piscitelli, A. Khaplanov, A. Devishvili, S. Schmidt, C. Höglund, J. Birch, A. J. C. Dennison, P. Gutfreund, R. Hall-Wilton, and P. Van Esch, Proc. R. Soc. A **472**, 20150711 (2016).
[27] E. H. Hauge and J. A. Støvneng, Rev. Mod. Phys. **61**, 917 (1989).
[28] M. Büttiker, Phys. Rev. B **27**, 6178 (1983).
[29] S. J. Blundell and J. A. C. Bland, Phys. Rev. B **46**, 3391 (1992).
[30] N. Pleshanov, Z. Phys. B Condens Matter **100**, 423 (1996).
[31] D. Krause, E. Fischbach, and Z. Rohrbach, Phys. Lett. A **378**, 2490 (2014).
[32] D. Karamitros, T. McKelvey, and A. Pilaftsis, Phys. Rev. D **108**, 016006 (2023).
[33] K. Artmann, Ann. Phys. (Berlin) **437**, 87 (1948).
[34] J. L. Carter and H. Hora, J. Opt. Soc. Am. **61**, 1640 (1971).
[35] V. Sears, Phys. Rep. **82**, 1 (1982).
[36] R. Van De Kruijs, V. Ul'yanov, M. Rekveldt, H. Fredrikze, N. Pleshanov, V. Pusenkov, V. Syromyatnikov, A. Schebetov, and S. Langridge, Physica (Amsterdam) **297B**, 180 (2001).
[37] R. Pynn *et al.*, RB2310511, STFC ISIS Facility (2023), 10.5286/ISIS.E.RB2310496.